Organic Vapor Sensing and Discrimination using Enhanced Sensitivity Thickness Shear Mode Devices

*Randolph D. Williams and Venkat R. Bhethanabotla**

Sensors Research Laboratory, ENB 118, Department of Chemical Engineering, University of South Florida, 4202 E. Fowler Ave., Tampa, FL 33620-5350, USA.

Abstract

Thickness shear mode (TSM) resonators, also known as quartz crystal micro-balances (QCM) are a class of acoustic wave sensors that have been used for gas/vapor sensing and for determining liquid properties. Fast and sensitive chemical vapor sensing, specifically of hydrocarbon vapors is the goal of this work. The TSM sensors typically used have a lower sensitivity compared with other acoustic wave sensors. This paper describes the development of high sensitivity organic vapor sensors using polymer thin film coatings of poly-isobutylene (PIB) on high frequency TSM devices. Commercially available AT-quartz TSM devices were milled to 17 μm, leaving a thin quartz membrane surrounded by a 50 μm thick outer ring. This resulted in an increased frequency and a consequent increase in sensitivity, as described by device models. TSM devices with fundamental mode resonant frequencies of 10, 20 MHz were compared to the milled 96 MHz devices. The organic vapors studied were benzene, toluene, n-hexane, cyclohexane, heptane, dichloroethane, dichloromethane, and chloroform at levels ranging from less than 1 to over 10 volume percentage in nitrogen gas. The Butterworth-VanDyke (BVD) equivalent circuit model was used to model both the perturbed and unperturbed TSM resonators. Monitoring the sensor response through the equivalent circuit model allowed for discriminating between the organic vapors. In particular, changes in the resistance parameter due to softening and relaxation of the PIB film allowed for this vapor discrimination. We present new results of tests conducted to demonstrate increase in sensitivity for higher fundamental frequency TSM devices. We evaluate and compare the performance of each sensor in terms of detection limit and noise level. We then suggest schemes for utilization of these sensors as continuous monitors for process vapor streams containing organic vapors of arbitrary concentration.

1. Introduction

TSM resonators with fundamental resonant frequencies of 5-20 MHz are typically utilized for sensing application. Such devices are limited in sensitivity because of their low resonant frequencies. Recently, high frequency TSM resonators with fundamental resonant frequencies of 100 MHz were fabricated by the inverse mesa technique; high frequency devices have never been tested in gas phase sensor applications [1, 2]. The objective of this work is to explore the possibility of utilizing these inverse mesa resonators as organic vapor sensors. Consequently, the higher frequency resonators were compared (in terms of sensor performance parameters) to 10 and 20 MHz resonators.

To construct gas or vapor sensors, chemically-sorbent films are commonly coated onto TSM resonators. Chemical sensitivity and selectivity is imparted by attaching a thin film to the acoustically active region of the TSM device. Devices employed in this work were AT-cut quartz crystals with circular gold electrodes on both sides. Because of the piezoelectric properties of the quartz material, application of a voltage between the two electrodes at the surface results in a shear deformation of the crystal. The quartz crystal then vibrates via the piezoelectric effect and this vibrational motion results in the generation of a transverse acoustic wave that propagates across the thickness of the quartz crystal. The resonant frequency of the TSM device decreases with the crystal thickness when a standing wave condition is met, as

$$t_q = \frac{\lambda_q}{2} \qquad (1)$$

$$v = \left(\frac{\mu_q}{\rho_q}\right)^{1/2} \qquad (2)$$

Here v is the velocity of sound in the quartz and t_q is the quartz thickness. Equation 2 gives the velocity, where ρ_q is the density (2.648 g cm^{-3}) and μ_q is the shear modulus (2.947 x 10^{11} g cm^{-1} s^{-2}) of the quartz. Since the quartz thickness is much larger than the electrode thickness, the electrodes are neglected when determining the resonant frequency. Equations have been developed to yield expressions for the dependence of the resonant frequency on the mass changes occurring within films coated onto the TSM sensor. The Sauerbrey equation is one such relationship, valid for small mass loadings, such as those occurring in vapor sensing applications:

$$\Delta f = \frac{2 f_r^{2} \Delta m}{(\mu_q \rho_q)^{1/2}} \qquad (3)$$

where Δf is the measured frequency shift, f_r is the resonant frequency, and Δm is the film areal mass density (which can be related to the film mass) [3]. Changes in the film mass will cause frequency shifts; these frequency shifts are dependent upon the film selectivity and the device sensitivity. In Sauerbrey's model, the sensitivity c_f is given by:

$$c_f = \frac{2 f_r^{2}}{\rho_q v_q} \qquad (4)$$

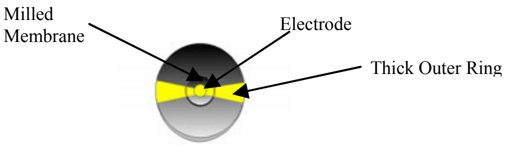

Figure 1. Milled TSM Device

Consequently, a commonly used 10 MHz AT-cut quartz crystal (with the previously mentioned physical properties) will have a mass sensitivity of 2.26 x 10^8 Hz cm^2 g^{-1}. Although a 10 MHz TSM sensor already has a high degree of theoretical sensitivity, it is obvious from equation 4 that this sensitivity can be considerably increased by increasing the resonant frequency. For a 56 MHz device, experimental sensitivity increases proportional to the 2.88 exponent of the resonant frequency have been reported for liquid sensing with the signal to noise ratio improving by a factor of 6.5 [4]. The plate thickness t_q determines the wavelength of the fundamental ($n = 1$) and harmonic ($n =$ 3, 5, 7 …) resonances as

$$f_n = \frac{nv}{2t_q} \qquad (5)$$

where f_n is the frequency of the nth harmonic. The design of high frequency resonators by milling techniques has been studied extensively [1, 5-7] . These higher frequency devices are long known to have improved mechanical stability and frequency to noise ratios that are better than other acoustic wave devices [8]. A diagram of a milled TSM device is shown in Figure 1. Milled TSM devices in this study had 96 MHz fundamental resonant frequencies.

2. Experimental Apparatus

The apparatus shown in Figure 2 was used to generate the organic vapors and to record the sensor responses to these vapors. The liquid solvents were housed in flasks maintained at 15 ˚C in the Vapor Generation section. Solvents were HPLC grade, obtained from various commercial sources, with 99.9 % purity. Solvent vapor pressures were calculated using Wagner's equation and the concentration of the generated vapor was varied by regulating the flow rate of the nitrogen gas with MKS mass flow controllers [9]. Solenoid valves were used to prevent cross mixing of solvents and to purge the system of any contaminants before testing. An Agilent 4294A precision impedance analyzer was used to monitor the resonant frequency and equivalent circuit parameters of the TSM devices. The sensor was located in a stainless steel test cell under temperature control (maintained at 22.5 ^{o}C). The apparatus was automated and controlled with Labview 7. The concentration of the generated vapors was calibrated gravimetrically with activated charcoal and found to be within 4-5 % of the calculated concentration. All crystals were AT-cut quartz with gold electrodes on a chromium adhesion layer. The milled membrane diameter of the 96 MHz device was approximately 0.127 cm. The 10 and 20 MHz devices were obtained from International Crystal Manufacturing. The 96 MHz devices were specially fabricated at MTronPTI, Orlando, FL, using chemical milling. The resonator quartz blanks were etched in NaOH.0.5H_2O at 180 ^{o}C. Additionally, these resonators were fabricated with ring thicknesses of approximately 50 µm and membrane thicknesses of approximately 17 µm. TSM devices were spray coated with PIB by utilizing an air brush [10].

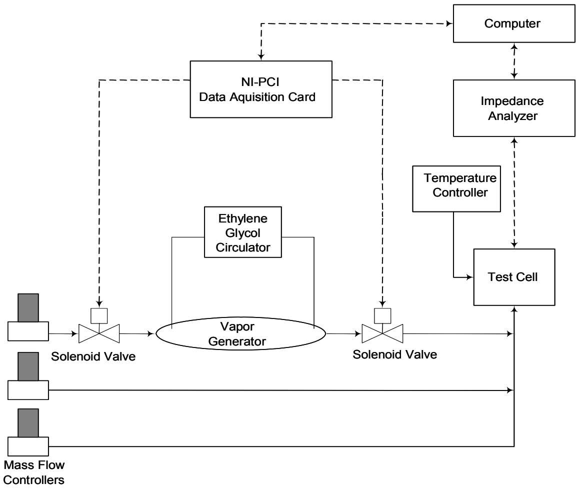

Figure 2. Vapor generating apparatus

3. Results and Discussion

We present detailed results for a PIB sensing film tested with benzene analyte. This typical case of an organic solvent, benzene, and a rubbery polymer is chosen to evaluate the dependence of sensor parameters on frequency. Each of the resonators was exposed to various concentrations of benzene. The vapor phase concentration was increased from 27,557 mg/m^3 to 232,688 mg/m^3, with purges of pure nitrogen gas between each exposure to allow the benzene vapor to desorb and the film to recover. A total flow rate of 100 ±1 sccm was always maintained over the surface of the device. Film thickness of the coated polymer and associated frequency shift for each resonator are given in Table 1. The ratio of the polymer film to the quartz membrane thickness is kept below 1% to stay within the mass balance regime within which Sauerbrey's equation is known to be valid for inertially coupled layers. Also, sensor response dampens as the polymer film thickness is increased, such that a limit of sensing film thickness exists for each sensor of a given fundamental resonant frequency. Since different resonators have different blank thicknesses, the thickness of the polymer sensing film cannot be constant.

Table 1. Polymer film parameters

Resonator Fequency (MHz)	Film Thickness *(nm)*	Frequency Shift (*kHz*)	Thickness Ratio (*percent*)
9.99325	961	20,112	0.58
19.99340	420	34,440	0.50
96.88852	141	275,413	0.82

The ratio of the thickness of the quartz blank to the thickness of the film can be kept at a near constant ratio, to facilitate more rational comparison of sensor response parameters. However, due to the higher sensitivity of the 96 MHz device, this constancy was difficult to achieve, leading to a slightly higher value, but still within 1%. In the experiments conducted, the responses of each resonator to various concentrations of benzene were recorded. From these data various sensor response parameters were determined and compared.

3.1 Sensor Response, Repeatability, Dynamic Range, L.O.D., Response and Recovery Time

Figure 3 demonstrates that the resonator responses (frequency changes) due to exposure to the analyte are repeatable. Each trial consisted of 1200 seconds of an initial purge with ultra high purity nitrogen, after which exposure and purge times were of 600 seconds duration each. The procedure was chosen to demonstrate the viability of the resonator as a sensor in terms of recovery after exposure to the test sample. Repeated cycling and re- testing of the polymer coated devices after several weeks yielded the same results. The inherent increase in sensitivity of the 96 MHz resonator, due to the increase in resonant frequency, is demonstrated by a comparison of the sensor response from each resonator, as shown in Figure 3 (d).

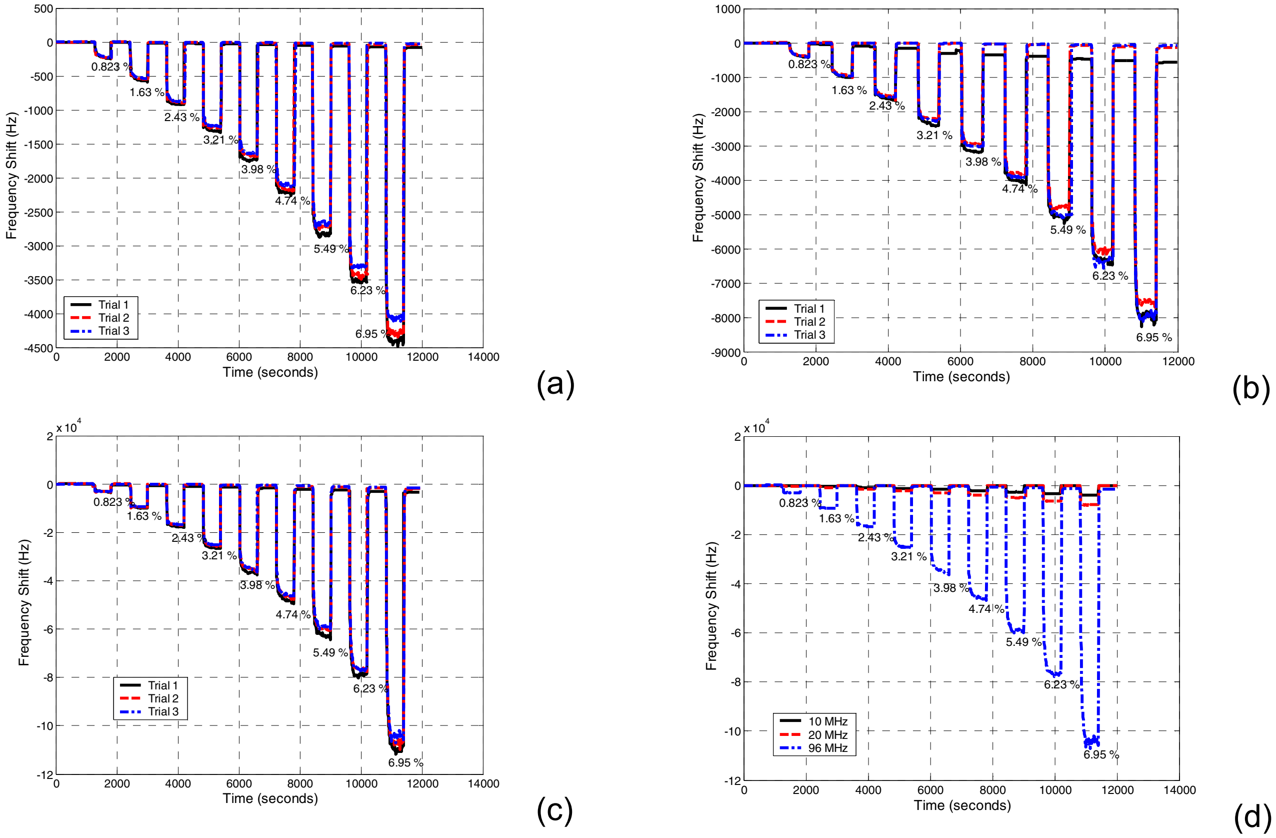

Figure 3. Repeatable sensor responses for the 10 (a), 20 (b) and 96 (c) MHz devices with a comparison of all sensor responses (d)

The base line drift for the 10 MHz device over the duration of the entire experiment of 12,000 seconds was 49 Hz. The 20 MHz and 96 MHz resonators had higher baseline drifts of 260 Hz and 2342 Hz, respectively. The baseline drift was probably the result of de-wetting effects. De-wetting affects the shape of a thin film polymer by reducing the area of the film/surface interface. During exposure to the analyte the polymer film likely breaks up into beads of isolated droplets. This effect was also observed during the coating procedure and has also been noted in previous studies[11].

Table 2. Dynamic range of TSM devices for several organic vapors

	Dynamic Range *(mg/m^3)*		
Chemical	10 MHz	20 MHz	96 MHz
Benzene	132 - 231371	267 - 255094	256 - 231371
Toluene	78 – 51,404	134 - 59840	40 - 59840
n-Hexane	334 - 335614	451 - 420444	431 - 335614
Heptane	99 - 106830	137 - 136371	49 - 106830
Cyclohexane	184 - 232945	161 - 286494	88 - 232945
Dichloroethane	1140 - 1300020	1940 - 1300020	88 - 1300020
Dichloromethane	957 - 265623	161 - 265623	100 - 265623
Chloroform	461 - 693076	626 - 766560	393 - 693076

Table 2 shows the dynamic range of eight organic vapors. These ranges are useful in considering the TSM devices as process stream concentration monitors. All of the tested organic solvents are reasonably soluble in the rubbery polymer poly(isobutylene), although frequency shifts at exposures of same concentrations are different for different organics, allowing for possibility of discrimination. We present results for the typical case of benzene, however, sensor response parameters for the other organics led to similar conclusions, hence, they are not presented in this paper.

The limit of detection (L.O.D.) and the noise level for each resonator was also determined from the sensor responses. Similar to the baseline drift, the frequency noise increased with the fundamental frequency of the resonators. The frequency noise is important since it determines the detection limit for the sensor. The frequency noise was defined as the standard deviation (S.D.) of the mean resonant frequency taken over a 7 minute interval in the presence of 100 sccm of pure nitrogen gas flow. The L.O.D. was determined to be 245, 268, and 256 *mg/m^3* for the 10, 20 and 96 MHz resonators respectively (calculated from 3S.D./Noise which is a 99 % confidence interval). The poor L.O.D. of the 96 MHz device, in comparison with the 10 MHz device, was due to the high noise levels of the 96 MHz device.

Values for the full response was established from a criterion of fluctuations around a mean value, and time constants for 63%, 95% and 99% sensor response were calculated. The 63% response time is between 10 and 20 seconds for all three sensors, except at the lowest concentration tested, where, the higher frequency device responds more quickly. The 99% response times also show a decreasing trend with concentration for all devices, with the 96 MHz device showing smaller times. These results are consistent with unsteady-state diffusion behavior in a polymer slab, however, smooth and monotonic decrease of the response times with increasing benzene concentration is not seen. This could be due to the non-uniform nature of the polymer film, and the complex nature of the diffusion process in these films. Recovery is relatively quick with 100 to 180 seconds for 99% recovery seen for all devices over the concentration range studied, with the 96 MHz device recovering quicker than the lower frequency ones.

3.2 Sensitivity

Sauerbrey’s model (equation 3) can be utilized to calculate the theoretically expected sensitivity for this polymer sorption process for each of the tested devices. This model provides an expression for frequency sensitivity to areal mass density (mass/unit active area of crystal), however, the active area is not exactly known. Hence, comparison with theory becomes convenient if an experimental sensitivity to areal mass density were expressed in terms of easily measured parameters. To establish if each of the three devices tested behaves according to Sauerbrey's model, we derive an expression for the experimental sensitivity in the following way. The frequency shift due to the polymer and sorbed solvent in the sensing film for each exposure is:

$$\Delta f = \Delta f_p + \Delta f_s \tag{6}$$

where Δf_p is the frequency shift due to the polymer and Δf_s is the frequency shift due to the solvent (analyte). Similarly, the areal mass density (mass/unit area) of the polymer/solvent sensing layer is given by:

$$\Delta m = \Delta m_p + \Delta m_s \tag{7}$$

We can define weight fraction of solvent in the polymer, w_s, in terms of the areal mass densities as:

$$w_s = \frac{\Delta m_s}{\Delta m_p + \Delta m_s} \tag{8}$$

Rearranging for $\Delta m_s + \Delta m_p$

$$\Delta m_s + \Delta m_p = \Delta m_p \left(\frac{1}{1 - w_s} \right) \tag{9}$$

Noting that the polymer film areal mass density equals $h\rho_p$, the product of the film thickness and polymer density, we have

$$\Delta m_p + \Delta m_s = h\rho_p \left(\frac{1}{1 - w_s} \right) \tag{10}$$

The sensitivity becomes

$$c_{fe} = \frac{\Delta f_p + \Delta f_s}{h\rho_p \left(\frac{1}{1 - w_s} \right)} \tag{11}$$

This expression can be utilized for calculating experimental mass sensitivity as it involves no determination of actual mass loaded on the crystal. The weight fractions were determined from frequency shifts by application of Sauerbrey's model to this 10 MHz device *via*

$$w_s = \frac{\Delta m_s}{\Delta m_p + \Delta m_s} = \frac{\Delta f_s}{\Delta f_p + \Delta f_s} \tag{12}$$

Finally, the polymer thickness *h* was determined by profilometer measurements, as well as from measured frequency shifts Δf_p and application of Sauerbrey's model for each device, before exposures to solvents. Poly(isobutylene) density was taken as 0.92 gm/cm^3, as given by the supplier Acros. Experimental sensitivities for the devices were concentration dependent, more so for the 96 MHz device. Sauerbrey's model predicts 4-fold and 92-fold increases in areal sensitivity for the 20 and 96 MHz devices in comparison to the 10 MHz device. From the experimental data, we find that these ratios range from 4.01 to 4.05, and 111 to 126, for the 20 and 96 MHz devices, respectively. From linear regression at each vapor exposure concentration, we can establish whether the f^2 dependence predicted by Sauerbrey's model is borne out. We find that the exponent is close to 2, varying between 2.08 to 2.14, in going from the lowest to the highest exposure concentrations of benzene vapor.

Figure 4 shows the calibration and device sensitivity plots as functions of vapor phase concentration for the three sensors studied. The device sensitivity is the first derivative of the calibration curve, and is simply the change in device frequency per unit change in vapor phase concentration. The calibration curves are represented very well by a quadratic function of the form

$$\Delta f = aC^2 + bC \qquad (13)$$

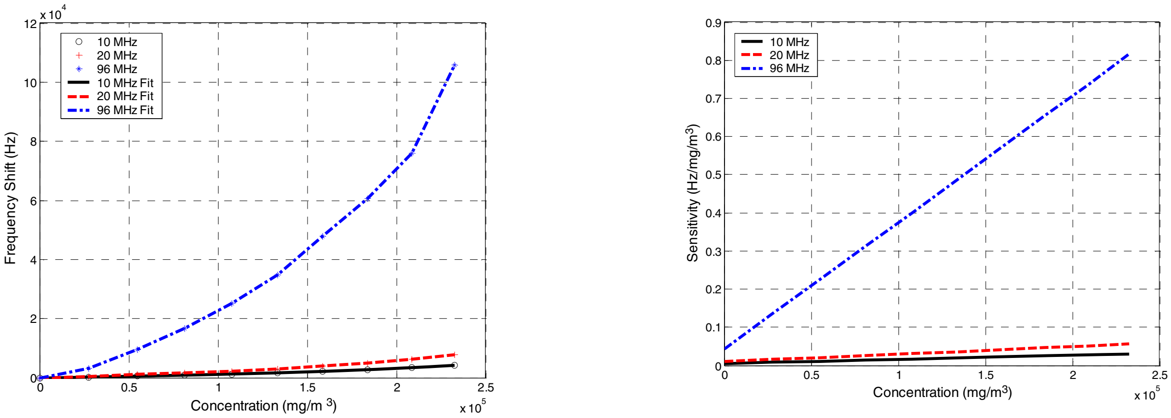

Figure 4. Calibration and sensitivity of the three sensors as functions of vapor phase concentration

Where Δf is the frequency shift that results from solvent exposure, and C is the vapor phase concentration of the analyte. For the 10 MHz device, A= 5.390 x 10^{-8} and B= 5.439 x 10^{-3}; for the 20 MHz device A= 9.839 x $10^{-8}$and B=1.008 x 10^{-3}; for the 96 MHz device, A= 1.661 x 10^{-6} and B=4.280 x 10^{-2}. Device sensitivity is seen to be linear in concentration, with a larger slope for the 96 MHz device indicating that this device can be utilized very well as a process monitor for higher concentrations of analyte, in addition to being useful as a low concentration detector (such as in lower explosion limit detection safety applications). Note that the device sensitivity of the 96 MHz sensor is 7.9 times that of the 10 MHz device at the lowest end of the concentration range, and is nearly 27 times that of the 10 MHz device at the highest concentration studied (2.33 x 10^5 mg/m^3). The device sensitivity ratio can be estimated from Sauerbrey's model to be a factor of 92 times the ratio of the film thicknesses, which are 961 and 141 nm, for the 10 and 96 MHz devices, respectively. This yields a constant value of 13.5 across the concentration range. In contrast, the observed values vary from 7.9 to 27. Part of the discrepancy at the lower concentration end can be explained by the uncertainty in determining the polymer film thickness, especially on the 96 MHz device. At the higher end, it is the deviation of the device response characteristics from Sauerbrey's model (viscoelastic effects) for the 96 MHz device that likely explain the difference.

3.3 Vapor Discrimination

The Agilent 4294A impedance analyzer was used to monitor the resistance parameter of the equivalent circuit model of the TSM sensor. Resistance changes due to changes in the polymer viscoelastic properties have been reported previously [12]. The resistance changes (along with changes in resonant frequency) may be unique to a particular solvent concentration and polymer film; consequently, resistance changes can be used to discriminate between vapors as shown in Figure. 5. Resistance changes for all solvents were measured over several trials and found to be constant at each concentration. For the four solvents in Figure 5, it is clear that the low levels (98460 mg/m^3) of chloroform can be distinguished from vapors of cyclohexane, heptane and toluene. Error bars represent the deviation in the total mean resistance and frequency change, due exposure to a vapors, over two trials. Vapor levels of TOL, HEP, CHX, and CLF above 34421, 61713, 120412 and 372074 mg/m^3 respectively can be discriminated. Vapor pairs of benzene and heptane, hexane and toluene, and dichloroethane and cyclohexane cannot be discriminated from changes in the resistance and resonant frequency.

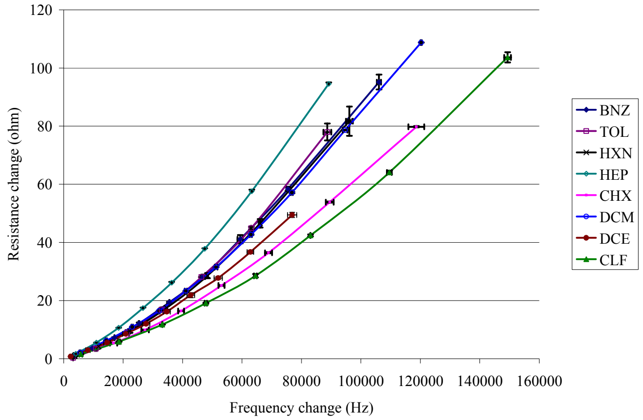

Figure. 5. Vapor Discrimination of cyclohexane, chloroform, heptane and toluene.

4. Conclusions

We conclude that milled TSM resonators with increased fundamental resonant frequencies can be utilized as improved organic vapor sensors both in a detection mode and in process stream monitoring applications. Significant improvements to the device sensitivity are realized compared to the lower frequency devices. Sensitivity was found to be analyte concentration dependent. L.O.D. for the higher frequency device was found to be comparable to the lower frequency ones. Response times were shorter for the higher frequency device, with a decreasing trend with analyte concentration for all devices. Recovery times were small for all devices and increased with analyte concentration. Sensor frequency response magnitudes compared reasonably well with the perturbation model of Sauerbrey, with larger deviations observed at higher vapor concentrations. Monitoring the resistance parameter of the BVD circuit allowed for vapor discrimination between selected solvents, showing which systems could be distinguished with poly(isobutylene) at room temperature. Finally, high frequency devices have advantages of simpler electronics, easier design and fabrication, well-developed models and good baseline stability compared to other acoustic wave devices.

5. References

*Corresponding author email: Venkat@eng.usf.edu

[1] J. R. Hunt., R. C. Smythe, Chemically milled VHF and UHF AT-cut resonators, In Proceedings of the 39th Annual Frequency Control Symposium (1986) 292-300.

[2] M. D. Ward, L. Zuxuan, C. M. Yip, I. S. Joseph, Operation of an ultrasensitive 30 MHz quartz microbalance in liquids, Anal. Chem., 65 (1993) 1546-1551.

[3] G. Sauerbrey, The use of quartz oscillators for weighing thin films and for microweighing, Zeitschrift fur Physik, (1959) 206-222.

[4] E. Uttenthaler, M. Schraml, J. Mandel, S. Drost, Ultrasensitive quartz crystal microbalance sensors for detection of M13-phages in liquids, Biosensors and Bioelectronics, 16 (2001) 735-743.

[5] J. R. Vig, J. W. Lebus, R. L. Filler, Chemically polished quartz, Proc. on the 31st Annual Symposium on Frequency Control (1977) 131-143.

[6] R. W. Ward, Etching of quartz crystal spheres, Salt Lake City, Utah, 1993 IEEE International Frequency Control Symposium (1993) 390-396.

[7] J. R. Vig, J. Ballato, R. E. Riman, S. Laffey, Etching Quartz Crystals in Anhydrous HF Gas, 1996 IEEE International Frequency Control Symposium (1996) 201-208.

[8] G. K. Guttwein, A. D. Ballato, T. J. Lukaszek, VHF-UHF Piezoelectric Resonators. US Patent 3694677, USA, (1972).

[9] R. C. Reid, J. M. Prausnitz, B. E. Poling, The Properties of Liquids and Gases, McGraw Hill, New York, 1987.

[10] D. S. Ballantine, R. M. White, S. J. Martin, A. J. Ricco, E. T. Zellers, G. C. Frye, H. Wohltjen, Acoustic wave sensors: theory, design, and physico-chemical applications, Academic Press, San Diego, 1997.

[11] J. W. Grate, A. R. McGill, Dewetting effects on polymer coated surface acoustic wave vapor sensors, Anal. Chem., 67 (1995) 4015-4019.

[12] A. F Holloway, A. Nabok, M. Thompson, A.K. Ray, T. Wilkop, Impedance analysis of the thickness shear mode resonator for organic vapour sensing, Sensors and Actuators B, 99 (2004) 355-360.